IOSR Journal of Applied Chemistry (IOSR-JAC)
e-ISSN: 2278-5736.Volume 10, Issue 6 Ver. I (June. 2017), PP 38-43
www.iosrjournals.org

Synthesis and Characterization of Samarium doped $SrBi_{2-x}O_4$ oxides

K. Chandru[1], G. Selvanathan[1], B.B. Das[2]
[1]*Department of Chemistry, A.V.C College (Autonomous), Mannampandal, Mayiladuthurai-609305, TN*
[2]*Functional Materials Chemistry Laboratory, Department of Chemistry, Pondicherry University, Puducherry-605014*

Abstract: *Sm^{3+} doped $SrBi_{2-x}O_4$ oxides were prepared by sol - gel method via nitrate citrate route with 'x' values ranging from 0.0, 0.1, 0.2, 0.3, and 0.4 (samples C0 - C4). X-ray powder diffraction analysis reveals the single phase monoclinic structure with the space group of P/2m. Rietveld refinement of unit cell structure shows lowered agreement factors R_p , R_{wp} and R_{exp} for all the samples. Average crystallite size was determined by Scherrer's relation in the range of ~36 - 45nm. Magnetic properties of the samples were analyzed by using Vibrating Sample Magnetometer at room temperature which reveals a weak ferromagnetic behaviour for C1 to C4 and diamagnetic behaviour for sample C0. EPR studies recorded at liquid helium temperature show a single absorption peak with defect line content. Optical absorption spectra of the prepared samples were recorded in UV visible region from 200nm to 800nm. FT-IR spectra of the samples were recorded at room temperature, which show the characteristic absorptions at 853 cm^{-1} and 533 cm^{-1} corresponding to the tetrahedral and octahedral sites. SEM studies show the particles were agglomerated with rod like structure. The combined TGA – DSC measurements show important stages of decomposition with no phase transition.*

Keywords: *Powder X-ray diffraction, Samarium ion, TGA, FT-IR, Sol – gel synthesis.*

I. Introduction

Growing demand for new research material with practical application necessity is growing everyday in view of scientific and technological interests. If a material is magnetically active nano metal oxide, it receives much attention owing to their application in memory storage device, data writing, gas sensors and in magnetic drug delivery system [1-2]. Choosing suitable magnetically active ion with excellent electrical and optical properties, one can cater the needs of growing demands. Rare earth ion with unpaired *4f* electron when doped in to larger size cation leads to significant structural distortion with strain and modifies the electrical and magnetic properties [3-6]. The method of preparation of this composite oxide material should involve low temperature, homogenous particles in nano range and good stoichiometric control. Several soft methods are available for the synthesis of magnetically active composite oxide material such as hydrothermal, micro emulsion, spray drying, sol – gel and reverse micelle method. Among these methods the sol – gel method [7] is one of the best method for preparing magnetically active composite oxide material which has the ability to provide all the desired properties.

II. Experimental

The sol-gel method was used for the synthesis of Sm^{3+} doped $SrBi_{2-x}O_4$ oxides. Sm^{3+} doped samples were synthesized by mixing $SrCO_3$, Sm_2O_3 and $Bi(NO_3)_2$ in a stiochiometric ratio to obtain $SrSm_xBi_{2-x}O_4$ oxides with x values from 0, 0.1, 0.2, 0.3, 0.4. Starting materials $SrCO_3$, Sm_2O_3 and $Bi(NO_3)_2$ were first mixed with aqueous HNO_3 solution (pH ~ 2) for converting into corresponding nitrates. In addition to nitric acid, urea was also added to Sm_2O_3 solution to act as a trigger during combustion process. The above said solution was mixed with 30 ml of 1.5 M citric acid and kept in magnetic stirrer at 50 °C for four days. The resulted gel like substance was then decomposed at 120 °C and sintered at 400 °C for 2 hours and then at 800 °C for 4 hours in a muffle furnace. The resulting powder obtained was ground in an agate mortar and utilized for characterization.

2.1. Characterization

X-ray powder diffraction studies were carried out in an X'pert powder X-ray diffractometer (PAN Analytical make) with a scan rate 27° / minute in the range of 10° – 75° in 2θ. Monochromatic Cu K_α radiation (λ~1.54060 Å) was used as X-ray source with a power 40 kV/30mA. Rietveld refinement method was used for the refinement of unit cell structure. FT-IR spectra are recorded using Thermo Scientific FT-IR spectrometer in the range 4000 – 450 cm^{-1}. Surface structure and particle morphology was studied using SEM (JSM – 5410). Optical absorption spectrum was recorded in a UV – Vis spectral region of 200 – 800 nm (UV 2450 Make: Shimadzu). Hitchi S – 3400 instrument was used for elemental analysis. Magnetic hysteresis measurements were made by using Vibrating Sample Magnetometer at room temperature (Make: Lake Shore, Model: 7404).

EPR spectra were recorded in a Bruker spectrometer in the X Band at Liquid helium with a temperature range of 6 – 70K. TGA measurement were recorded by using TA instruments (Model: Q600 and Q20 DSC). Density measurements were done by using liquid displacement method using Carbon tetrachloride as an immersion liquid (density 1.596 g/cc at 300K)

III. Results And Discussion

3.1. X – ray diffraction studies

XRD patterns of prepared samples with different doping amount of Sm^{3+} ions are given in figure-1. Sharp diffraction peaks are observed for XRD pattern of C0 to C4. Multiplets of peaks from C1 to C4 indicate the successful incorporation of Sm^{3+} ion. The doping of Sm^{3+} ion (0.964 Å) which has smaller ionic radius than Bi^{3+} (1.03 Å), as a result it leads to structural distortion in the lattice sites [8-10]. Cell volume increases for concentration C0 to C2 and decline for C3 and C4. Average crystallite size is calculated by Scherrer formula and found to be in the range of 36 to 45nm. Though the compositional formula of $SrBi_2O_4$ represents spinel oxide formula AB_2O_4, $SrBi_2O_4$ is a non spinel oxide which crystallizes in monoclinic state as reported earlier [11-12]. Structural investigations using standard Rietveld Profile refinement indicate monoclinic phase with no other secondary phase having a space group of P / 2m, which is in agreement with the respective joint committee on powder diffraction standards. The agreement factors after Rietveld refinement of unit cell structure of $SrSm_xBi_{2-x}O_4$ are given in the table 1.

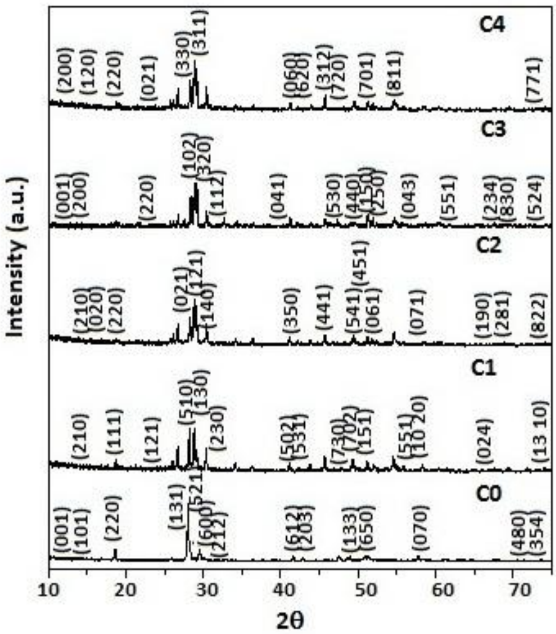

Fig. 1. Powder X-ray diffraction patterns of Sm^{3+} substituted $SrBi_{2-2x}O_4$ samples C0 to C4

Agreement Factors			
Sample ID	R_p (%)	R_{wp} (%)	R_{exp} (%)
C0	100.63	98.82	0.06
C1	95.79	94.38	0.07
C2	97.14	97.18	0.08
C3	91.92	99.88	0.09
C4	97.42	96.17	0.06

Table. 1. Agreement factors after Rietveld refinement of $SrSm_xBi_{2-x}O_4$ unit cell structure

3.2. Thermal analysis

From TG curve, it is evident that weight loss starts gradually from room temperature (Fig. 2). First stage of decomposition starts from room temperature to 400°C which might be due to elimination of trapped water molecule. In general sol gel method shows weight loss due to dehydration by 5% [13]. In second stage, there is a slight weight loss at 400°C which is due to removal of oxygen present in the sample. To conclude there is no significant thermal change and the compound is thermally stable up to 800°C.

DOI: 10.9790/5736-1006013843

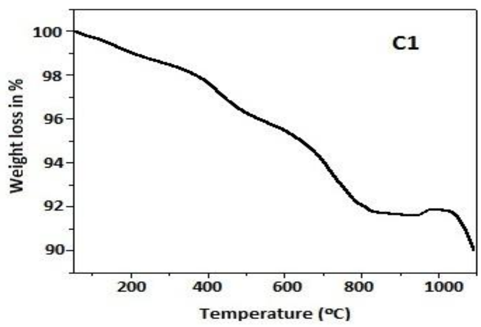

Fig. 2. TG curve of $SrBi_2O_4:Sm^{3+}$ for $x = 0.15$

3.3. SEM and Elemental analysis

Scanning electron micrograph and EDX of prepared samples are shown in the figure-3. Nature of Sm^{3+} doped $SrBi_{2-x}O_4$ oxide shows nano rod formation for C0. From C1 to C4 agglomeration can be seen for the prepared samples with the increase in concentration of Sm^{3+} ion. Incorporation of samarium ion in the lattice reduces the pores and void present in the lattice structure. Elemental analysis confirms the presence of oxygen, samarium, strontium and bismuth in the stoichiometric proportion (Table 2). Elemental analysis results show that the prepared samples are free from impurity.

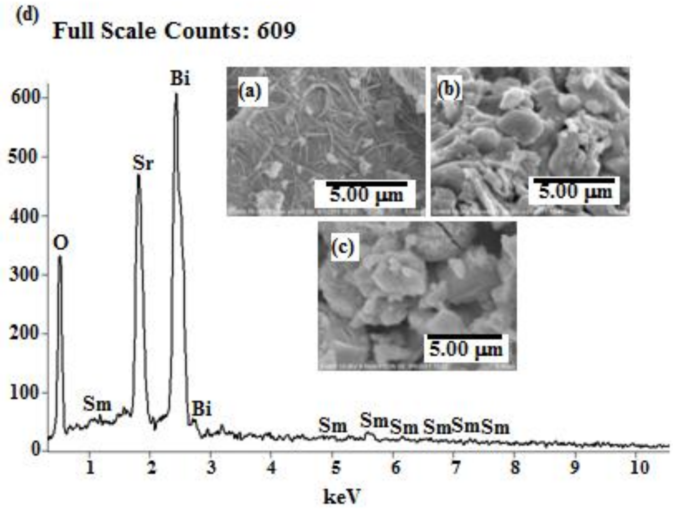

Fig.3. SEM images of (a) C0 (b) C1 (c) C4 at different magnification and (d) EDX profile of C1 with corresponding elemental composition values

Sample ID	Sr (wt %)	Sm (wt %)	Bi (wt %)	O (wt %)
C0	12.05	-	69.62	18.34
C1	17.94	3.77	49.13	29.15
C2	16.75	6.70	50.40	26.15
C3	16.21	12.08	46.91	24.80
C4	18.54	11.32	45.35	24.79

Table. 2. Elemental composition of prepared samples using EDX

3.4. UV-Visible absorption studies

UV-Vis absorption spectra of Sm^{3+} doped $SrBi_{2-x}O_4$ oxides for composition x = 0, 0.1 and 0.2 is shown in figure-4. Sm^{3+} doped $SrBi_{2-x}O_4$ oxides shows optical absorption in the range 350 - 400nm. As the concentration of Sm^{3+} increases, absorption shows a mild shift to longer wavelength. This is due to the charge transfer from *2p* orbital of oxygen atom to *4f* orbital of Sm^{3+} ion. Undoped $SrBi_{2-x}O_4$ shows absorption at 340nm and substitution of Sm^{3+} increases the absorption wavelength to 410nm.

.

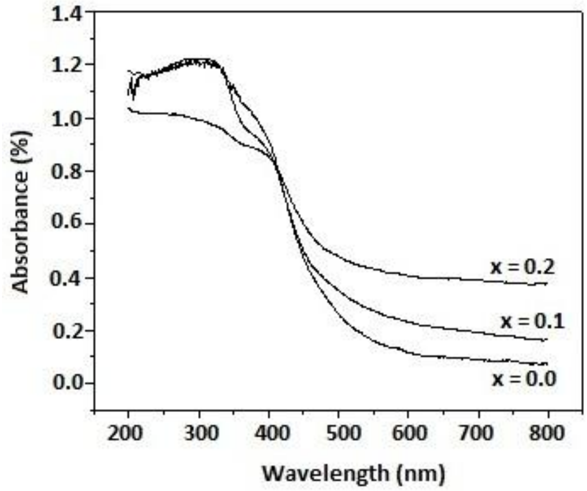

Fig. 4. UV-Vis absorption spectra of Sm^{3+} doped $SrBi_{2-x}O_4$ oxides

3.5. Fourier Transform Infrared

A representative FT-IR spectrum is given in the figure-5 for sample C3. Broad band in the range 3124 cm^{-1} is assigned to stretching mode of OH group and absorption in the range 1766 cm^{-1} assigned to bending mode of OH group. Vibration around 1470 cm^{-1} to 1390 cm^{-1} assigned to antisymmetric NO stretching vibration because of residual nitrate present in the sample [14]. In the region less than 1000 cm^{-1} there are absorption band at 906 cm^{-1}, 853 cm^{-1}, 703 cm^{-1}, 629 cm^{-1} and 553 cm^{-1}. Absorption at 533 and 629 cm^{-1} is due to Bi-O stretching vibration at $[BiO_6]$ units at octahedral sites and weak shoulder at 703 cm^{-1} corresponds to symmetric stretching vibration of Bi-O bond in pyramidal $[BiO_3]$ units [14,15]. Broad band at 853 cm^{-1} is assigned to Sr-O bond [12] or due to vibration of Sm^{3+}-O^{2-} bond [16].

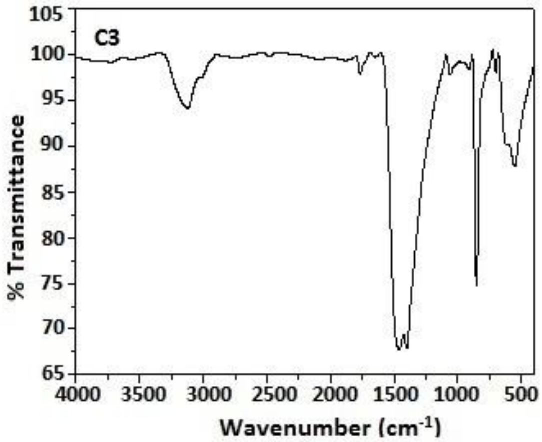

Fig. 5. FT-IR Spectra $SrSm_xBi_{2-x}O_4$ of sample C3 at room temperature

3.6. Magnetic measurements

Magnetic hysteresis loops of Sm^{3+} doped $SrBi_{2-x}O_4$ oxides C1 to C4 show a soft ferromagnetic behaviour at room temperature (Fig. 6 & 7). Sample C0 exhibit diamagnetic behaviour owing to the absence of Sm^{3+} ion as Sr^{2+} and Bi^{3+} shows diamagnetic character. Samples C1 to C4 show a weak ferromagnetic behaviour in the order of 10^{-3} emu/g which indicates successful incorporation of Sm^{3+} ion (Table 3). Paramagnetic nature of Sm^{3+} is mainly due to the presence of unpaired *4f* electron. From VSM figure, one can infer that ferromagnetic curve for x = 0.30 and 0.60 are very narrow which is due to low values of saturation magnetization *Ms* and magnetic remanence *Mr*. Increase in samarium concentration leads to the porosity which may be the reason for the declining *Ms* values. Also variation in *Ms* values are due to the different cation distribution and surface structural distortion. Variation in coercivity values are attributed to movement of domain walls in response to the magnetic field [17].

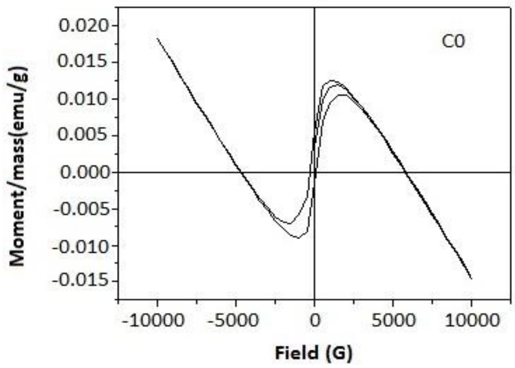

Fig. 6. Hysteresis loop showing diamagnetic behaviour of $SrBi_2O_4$

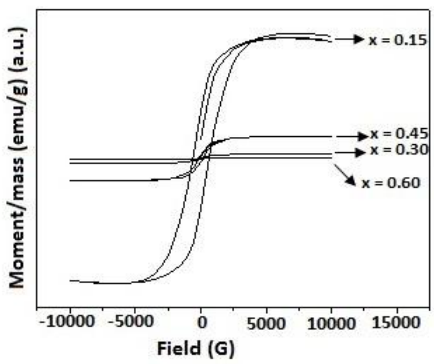

Fig.7. Hysteresis loop showing ferromagnetic behaviour of $SrSm_xBi_{2-x}O_4$ series

Sample ID	Magnetic Properties		
	Ms (emu/g)	*Mr* (emu/g)	*Hc* (G)
C0	16.446×10^{-3}	3.527×10^{-3}	3069.5
C1	18.908×10^{-3}	7.342×10^{-3}	597.37
C2	0.754×10^{-3}	0.050×10^{-3}	70.073
C3	3.366×10^{-3}	0.523×10^{-3}	151.85
C4	0.147×10^{-3}	0.013×10^{-3}	83.332

Table 3. Magnetisation values of $SrSm_xBi_{2-x}O_4$

3.7. EPR studies

Figure-5 shows EPR spectra of Sm^{3+} doped $SrBi_2O_4$ oxide with x = 0.30 at 93 K. Electronic configuration of Sm^{3+} is $4f^5$. Rare earth ion with half filled *4f* shell is strongly coupled to lattice fluctuations except Gd^{3+} ion with $4f^5$ configuration. Due to this, these ions have short spin-lattice relaxation times and as a result, EPR spectra can be observed only at low liquid helium temperature. From the EPR spectra, we can observe two absorption signals. First absorption signal at g ~ 1.9 is weak, less intense and broadened due to unresolved hyperfine splitting which indicate the presence of paramagnetic site due to Sm^{3+} ion [18-20]. Second absorption signal at g ~4.2 to 4.8 is broad, unresolved giving a long shoulder like structure.

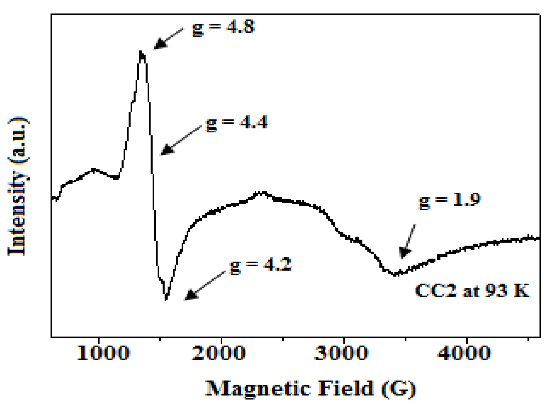

Fig.7. EPR Spectra of Sm^{3+} doped $SrSm_xBi_xO_4$ oxide at Liquid helium temperature when x = 0.2

IV. Conclusion

Sm^{3+} doped $SrBi_2O_4$ oxides with varying composition were synthesized by sol gel method. Powder XRD analysis confirms the presence of monoclinic structure with space group P / 2m. TGA-DSC reveals no significant weight loss and all the samples are thermally stable up to 800 ^oC. FT-IR analysis confirms the stretching vibration of Bi-O bond in octahedral coordination sites. EPR studies reveal weak paramagnetic absorption with g ~1.9 with defect line content. Scanning electron microscope shows grains which are agglomerated with irregular particle size. UV-Vis absorption studies shows absorption in the range 350-400nm. Magnetic behaviour of samples shows weak ferromagnetic of the order of 10^{-3} emu/g. Decrease in magnetic values is due to increase in samarium concentration which reduces magnetic behaviour between strontium and bismuth sites.

References

[1] P.A. Shaikh, R.C. Kambale, A.V. Rao and Y.D. Kolekar, Structural, magnetic and electrical properties of Co–Ni–Mn ferrites synthesized by co-precipitation method, *Journal of Alloys and Compounds, 492(1-2)*, 2010, 590-596.

[2] X. Cao, G. Liu, Y. Wang, J. Li and R. Hong, Preparation of octahedral shaped $Mn_{0.8}Zn_{0.2}Fe_2O_4$ ferrites via co-precipitation *Journal of Alloys and Compounds, 497(1-2)*, 2010, L9-L12.

[3] H.N. Lee, D. Hesse, Anisotropic ferroelectric properties of epitaxially twinned $Bi_{3.25}La_{0.75}Ti_3O_{12}$ thin films grown with three different orientations, *Applied Physics Letters, 80(6),* 2002, 1040-1042.

[4] K.S. Nalwa, A. Garg, A. Upadhyaya, Effect of samarium doping on the properties of solid-state synthesized multiferroic bismuth ferrite, *Materials Letters, 62(6),* 2008, 878–881.

[5] Ge-Liang Sun, Jian-Bao Li, Jing-Jing Sun, Xiao-Zhan Yang, The influences of Zn^{2+} and some rare-earth ions on the magnetic properties of nickel–zinc ferrites, *Journal of Magnetism and Magnetic Materials, 281(2–3),* 2004, 173-177.

[6] N. Rezlescu, E. Rezlescu, C. Pasnicu and M.L.Craus, Effects of the rare-earth ions on some properties of a nickel-zinc ferrite, *Journal of Physics: Condensed Matter, 6,* 1994, 5707-5716.

[7] A. Mali and A. Ataie, Influence of Fe/Ba molar ratio on the characteristics of Ba-hexaferrite particles prepared by sol–gel combustion method, *Journal of Alloys and Compounds, 399(1-2)*, 2005, 245-250.

[8] G.S. Arya, R.K. Sharma, N.S. Negi, Enhanced magnetic properties of Sm and Mn co-doped $BiFeO_3$ nanoparticles at room temperature, *Materials Letters, 93,* 2013, 341–344.

[9] X. Xu, T. Guoqiang, R. Huijun, X. Ao, Structural, electric and multiferroic properties of Sm-doped $BiFeO_3$ thin films prepared by the sol–gel process, *Ceramics International, 39,* 2013, 6223–6228.

[10] D. Haiyang, C. Zhenping, L. Tao, L. Yong, Microstructure and properties of Sm-substituted $BiFeO_3$ ceramics, *Journal of Rare Earths, 30(11),* 2012, 1123–1128.

[11] J. Popović, B. Gržeta, B. Rakvin, E. Tkalčec, M. Vrankić, S. Kurajica, Partial inverse spinel structure of manganese-doped gahnite: XRD and EPR spectroscopy studies, *Journal of Alloys and Compounds, 509(34),* 2011, 8487-8492.

[12] H.G. Ahalya, B.H. Doreswamy, B.M. Nagabhushana, Synthesis and characterization of $SrAl_2O_4$: Sm phosphor by low temperature synthesis, *International Journal of Research in Engineering and Technology, 3(6),* 2014, 553- 557.

[13] J.H. Kim, H.D Jang, S.K. Kim, Photoluminescence and photocurrent characteristics of $Sr_{1-x}Ba_xAl_2O_4$: Eu^{2+}, Ni^{2+} phosphors, *Ceramics international, 38(S1),* 2012, S577-S580.

[14] M. Mallahi, A. Shokuhfar, M. R.Vaezi, A. Esmaeilirad, V. Mazinani, Synthesis and characterization of Bismuth oxide nanoparticles via sol-gel method, *American Journal of Engineering Research, 3(4),* 2014, 162-165.

[15] F. He, Z. He, J. Xie, Y. Li, IR and Raman Spectra Properties of Bi_2O_3-ZnO-B_2O_3-BaO Quaternary Glass System, *American Journal of Analytical Chemistry, 5(16)*, 2014, 1142-1150.

[16] M.M. Rashad, R.M. Mohamed, H. El-Shall, Magnetic properties of nanocrystalline Sm-substituted $CoFe_2O_4$ synthesized by citrate precursor method, *Journal of Materials Processing Technology, 198(1-3)*, 2008, 139-146

[17] T. Smitha, P.J. Binu, X. Sheena, E.M. Mohammed, Effect of samarium substitution on structural and magnetic properties of magnesium ferrite nanoparticles, *Journal of Magnetism and Magnetic Materials, 348,* 2013, 140–145

[18] S. Zhang, W. Li, Z. Jin, J. Yang, J. Zhang, Z. Du, Z. Zhang, Study on ESR and inter-related properties of vacuum-dehydrated nanotubed titanic acid, *Journal of Solid State Chemistry. 177(4-5),* 2004, 1365-1371.

[19] M. Sterrer, E. Fischbach, T. Risse, H. Freund, Geometric characterization of a singly charged oxygen vacancy on a single-crystalline MgO(001) film by electron paramagnetic resonance spectroscopy, *Physical Review Letters, 94,* 2005, 186101-4.

[20] G. Dong, X. Xiao, Y. Chi, B. Qian, X. Liu, Z. Ma, S. Ye, E. Wu, H. Zeng, D. Chen, and J.Qiu, Polarized luminescence properties of TiO_2:Sm^{3+} microfibers and microbelts prepared by electrospinning, *The Journal of Physical Chemistry C, 113(22),* 2009, 9595–9600